Available online at www.sciencedirect.com

SCIENCE DIRECT

Polymer 45 (2004) 8279–8297

polymer

www.elsevier.com/locate/polymer

Feature Article

Motion of nano-objects on polymer brushes

Svetlana Santer*[1], Jürgen Rühe

Chemistry and Physics at Interfaces, Institute for Microsystem Technology (IMTEK), University of Freiburg, Georges-Koehler-Allee 103, D-79110 Freiburg, Germany

Received 28 April 2004; received in revised form 1 September 2004; accepted 22 September 2004

Abstract

In this paper we review a new method to move nano-objects on a polymer surface that is made from diblock-copolymer and mixed brushes. Such brush systems consist of polymer chains covalently attached to a surface with high grafting density. If the two polymeric components the brush consists of are incompatible with each other, it shows microphase separation into nanopatterns of well defined size. Such a system possesses the unique property of changing the surface topography in response to different external conditions. Motion of nano objects adsorbed on the brush is induced by having the external conditions and thus the brush topography vary over time. This is shown by studying the distribution of silica nanoparticles adsorbed on several types of brushes while changing the external conditions. We identify parameters required for motion of nano objects, and discuss potential applications of the proposed technique for nano engineering.

Keywords: Application of diblock-copolymer and mixed brushes; Motion of nanoparticles

1. Interaction of nano-particles with polymer brushes

The literature on potential applications of polymer brushes covers a variety of important areas, such as colloid stabilization [1], chemical gates [2], drug delivery [3], biomimetic materials [4], and the modification of lubrication, friction, adhesion and wettability of surfaces [5–7]. With this paper, we demonstrate that the rich physical properties of polymer brushes may lead to intriguing applications in nanotechnology as well, namely transport of adsorbed nano-particles [8]. Before discussing the interaction of nanoparticles with polymer brushes and their motion on such surfaces, some general features of polymer brushes are briefly reviewed.

A polymer brush is generally built from an ensemble of polymer chains that are attached either chemically (through covalent bonding) [9] or physically (by physisorption) [10] with one end to a surface. When the concentration of attached chains increases, first partial and then significant overlapping of neighbouring chains occurs [11,12]. The interplay between the repulsion of the repeat units inside the brush and the elasticity of the polymer chains leads to stretching of the chains away from the surface [13]. This introduces new interesting physical properties so that polymer brushes behave very differently from simply adsorbed polymer chains [14–16]. To obtain thick polymer brushes with high grafting density, the so-called 'grafting from' synthesis protocol can be applied by which polymer chains are grown from initiators on the surface [17,18]. Concerning the synthesis and the properties of homopolymer brushes, several reviews are available [19].

Especially interesting systems are brushes consisting of two or three different components, in which phase separation can occur. Such systems may be classified into two categories: (i) brushes consisting of di- or tri-block copolymer chains with one end covalently attached to a solid substrate [20]; (ii) mixed brushes, composed of a mixture of two polymers A and B, attached randomly to a surface (Fig. 1) [21]. As is well known, block copolymers in general show microphase separation. On surfaces, together with covalent bonding, an even more complex phase separation behaviour is induced. It depends on surface characteristics such as grafting density, the surface energy of both blocks that are in contact with either air, solvent or

* Corresponding author. Tel.: +49 761 2037415; fax: +49 761 2037162.
E-mail address: prokhoro@imtek.de (S. Santer).
[1] Born Prokhorova.

0032-3861
doi:10.1016/j.polymer.2004.09.085

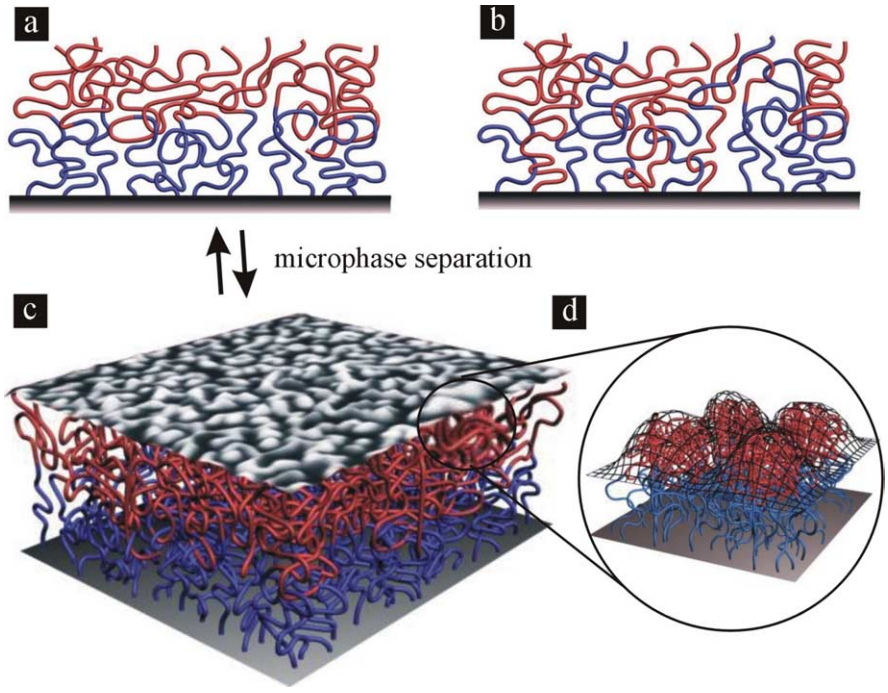

Fig. 1. Schematic depiction of the two types of polymer brushes: (a) diblock-copolymer brush, (b) mixed brush; (c) and (d) illustration of the nanophase separation into a structured topography for a diblock copolymer brush. Phase separation for the mixed brush proceeds along similar lines.

solid; and it additionally depends on specific molecular parameters such as the Flory–Huggings interaction parameter, and the molecular weight of the polymer chains [22]. By controlling all of these parameters, a variety of surface patterns consisting of characteristic structural elements can be obtained [22]. The patterns are not only topographical in nature; they also introduce variations in surface energy and chemical potential on a nanoscale. In that respect the term 'nanophase separation' would be more appropriate. For a given brush, the extent of this *nanophase separation* depends on the external conditions. By varying these, the brush can be reversibly switched from one pattern to an other.

Experimentally, the investigation of diblock-copolymer brushes started with the introduction of the atom transfer radical polymerisation (ATRP), which allows simple adjustment of structure and composition of the brush, and possesses the ability to prepare diblock copolymers by sequential activation of the dormant chain end in presence of different monomers [23–26]. Using AFM, Brittain et al. showed that PS-*b*-PMMA and PS-*b*-PMA diblock-copolymer brushes exhibit different morphologies, ranging from smooth to very rough surfaces, with either regular structure or with an unusual morphology, depending on the environment the film has been exposed to [27].

Another interesting system showing phase separation on a nanoscale is a mixed brush. Mixed brushes have been investigated with respect to structure formation during microphase separation as well [28,29]. One example of a mixed brush, a random copolymer of styrene and 2,3,4,5,6-pentafluorostyrene (PSF) and polymethylmethacrylate (PMMA), was shown to undergo transitions between a ripple-like topography and a dimple like structure [30], as was also predicted theoretically [31,32].

The studies carried out so far have mainly concentrated on identifying the different topographies of polymer brushes and elucidating how the brush structure influences the nanophase separation. This information is very important for some of the applications mentioned, such as designing smart surfaces that respond to external stimuli in order to change wettability and adhesion properties.

In addition to these applications of polymer brushes, they also possess properties rendering them interesting for the positional assembly of colloids [33,34]. The objectives of the studies are similar to those of traditional wet colloid chemistry, where short polymer chains such as bifunctional, self assembled monolayers immobilized on a surface are used as functional groups for the positional assembly of colloids [35].

To the best of our knowledge, only in a single publication polymer brushes of covalently bound poly(acryl amide), possessing a macroscopic gradient in molecular weight of the chains, were used as an organic template for the 3D spatial arrangement of gold particles [36,37]. Although the exact nature of the interaction force remains somewhat unclear, it was shown that at a given grafting density of the polymer brush, large gold particles (diameter $\sim$16 nm) predominantly stay near the brush/air interface, while smaller nano-particles (diameter $\sim$3.5 nm) penetrate deeper into the polymer brush, thus forming a 3D structure.

The case of non specific interactions of colloids with a brush, for which no positional assembly of the nanoparticles can be expected, was so far studied only for one example of thiol modified gold nanocrystals situated on a poly(ethyl-enepropylene) (PEP) brush. A PEP monolayer of 3 nm thickness was prepared by physisorption of a diblock copolymer poly(styrene-*b*-ethylenepropylene) (PS-PEP), throughout the PS block to an underlying polystyrene surface. The PS in turn was spin-coated on a layer of a poly(styrene-*b*-vinylpyridine) (PS-P2VP) diblock copolymer physisorbed to the surface of a silicon wafer [38]. It was found that brushes with a thickness less than the diameter of the nanoparticles inhibit their aggregation, while brushes with a thickness greater than the size of the gold particles mediate the formation of big islands with elongated shape. The interpretation of the results is not so straightforward as no information was provided on the microstructure of the rather complex underlying substrate.

Using the polymer brushes in order to move colloids adsorbed on their top is, however, a completely new aspect that is not covered in the research on polymer brushes so far. In the following we show that changes in the nanophase structure of such films can cause the nano particles to move on the surface. To put this new approach of moving nano particles into context, we shall also briefly comment on existing approaches for generating the movement of nano particles and for developing nano engines.

2. Motion of nanospheres on/by polymer brushes

2.1. Existing approaches for manipulating nano-particles on a surface

One of the challenging steps in performing complex operations on a nanoscale is to establish a nano infrastructure, i.e. providing facilities to move and arrange nano scale components. In order to drive or manipulate nano objects on surfaces, there are currently two major approaches, depending on the actuation mechanism: (i) moving nano objects or single atoms with a macroscopic device, such as an SFM probe tip [39], and (ii) nanomotors based on protein complexes [40]. In the former case, several groups have demonstrated that it is possible to arrange a small number of clusters or atoms on a flat surface in simple geometrical shapes, such as lines or squares [41]. Although this approach is very promising, it suffers from severe problems; the procedure is slow and difficult to perform, and accordingly it has low throughput and requires significant advances on automation of nano manipulation procedures for carrying it further [42]. The latter, seemingly general purpose approach utilizes 'walking' protein complexes such as kinesin/microtubules or myosin/actin. These complexes build the basis for contraction-expansion processes in muscle cells, transport of organelles, and segregation of chromosomes during mitosis. Those proteins convert chemical energy into mechanical work by ATP hydrolysis. Applications of these biological motors in nano engineering are intriguing, as they possess a high efficiency, are small and available in large numbers [43]. However, the specifics of the chemical process of how mechanical work is retrieved from chemically stored energy are still not well understood [44]. Even when these questions are answered satisfactorily, one has to take into account that protein complexes are fully functional only in buffered aqueous solutions, and only within a narrow temperature range. This significantly restricts their use in practical applications, e.g. when it is desired to integrate nano machines into electronic systems, where no aqueous environment is allowed.

Very recently, another approach was presented using carbon nanotubes together with scaled down existing micromechanical systems (MEMS). This is the first report on a fully synthetic nanoscale electromechanical actuator incorporating a rotating metal plate, with a multi-walled carbon nanotube serving as the key motion-enabling element [45].

In general, there may not be a single approach to nano manipulation that will be useful for all conceivable tasks. More likely there will always be a collection of different methods, according to their characteristic features. For instance, the approach to be outlined here could well provide the basis for an assembly line or conveyor belt for nano-objects, where on a suitably prepared surface a large number of objects can be moved simultaneously.

2.2. The concept of using a polymer brush to move nano-objects

In recent publications, we have proposed to use functional polymer films made of diblock-copolymer and mixed brushes to move nano-objects adsorbed on top of their surface (Fig. 2) [8,46,47]. The essential idea is that different topographical and chemical configurations of the polymer brushes together with drastic changes in surface energy and potential landscape during a phase transition, can cause the polymer chains to grasp or release a nano-object successively, moving it across a surface (Fig. 2).

Fig. 3 provides a simple picture how an elementary step of motion might occur. When a structure element (symbolized as a bump) is created during a phase transition, a nano object is moved out of its original location in the course of the transition. With the bump, we might associate a local excess value of, e.g. adhesion energy. Depending on the brush composition, in principle, different kinds of forces can be expected. However, the mechanism in Fig. 3 should not be mistaken with 'rolling down a hill', induced by the gravitational force, as its value, at the length scales considered here, is many orders of magnitude smaller than, e.g. surface forces. A more detailed discussion is carried out in Section 3.

In the following, the mechanism of motion is discussed with respect to a detailed account of nanophase separation

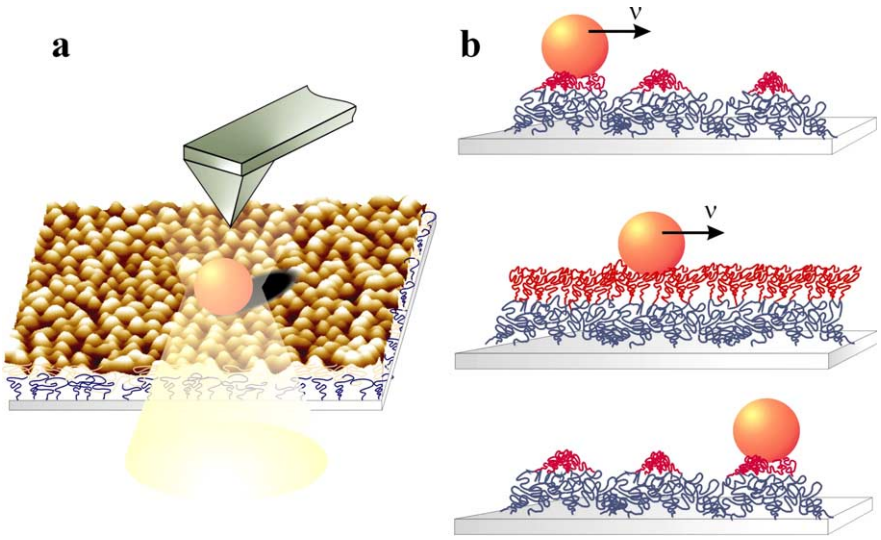

Fig. 2. (a) Scheme of a polymer brush carrying a cargo. (b) During topography switching accompanied by changes in the interfacial energy, the 'arms' of the brush grasp the nano cargo and move it along a surface.

of several kinds of polymer brushes. Two diblock-copolymer brushes (1) a poly(methylmethacrylate-b-glycidylmethacrylate) (p(MMA-*b*-GMA)), (2) a poly(benzyl-n-methacrylate-b-styrene) (p(BnMA-*b*-S)), and a mixed brush, consisting of polymethylmethacrylate and polyglycidylmethacrylate chains (PMMA-PGMA) are studied. Especially the behavior with respect to the switching process over many periods is presented ex-situ as well as in-situ.

2.3. Nanophase separation behavior of diblock-copolymer and mixed brushes

2.3.1. Ex-situ switching of brush topography in solvents

As a first step we studied the nanophase separation behavior of the diblock copolymer brushes. For the poly(methylmethacrylate-*b*-glycidylmethacrylate) brushes (PMMA-*b*-PGMA), PMMA was the attached block (Scheme 1). For the poly(benzyl-*n*-methacrylate-*b*-styrene) (p(BnMA-*b*-S)) brushes PBnMA was the attached block (Scheme 2). The PMMA and PBnMA macroinitiators were synthesized from a covalently attached 2-bromoisobutyrate initiator monolayer on the surface of a silicon wafer (Schemes 1 and 2) [48,49]. The initiator monolayer was formed under inert conditions at room temperature, using triethyl amine as a catalyst, toluene as solvent and a monochlorosilane group as the anchoring moiety. The polymers were grown from this surface attached initiator using ATRP at room temperature [48,49]. Thereafter, the PMMA and PBnMA brushes were used as a macroinitiator for the synthesis of the second blocks, namely the polyglycidylmethacrylate (PGMA) and polystyrene (PS) blocks, respectively. A more detailed description of the synthesis procedure is given elsewhere [48,49].

We studied a series of diblock copolymer brushes depicted in Schemes 1 and 2, differing in molecular weight of the first block, i.e. PMMA and PBnMA, respectively (Tables 1 and 2). The molecular weight of the second block (PGMA and PS) of each of the two systems was the same within each series. To be more precise, for the p(MMA-*b*-GMA) brush, the degree of polymerisation of the first block (DP_{PMMA}) ranged from 600 to 800, while the degree of polymerisation of the PGMA block (DP_{PGMA}) was 300 in all three cases (Table 1). For the p(BnMA-*b*-S) diblock-copolymer brush, the degree of polymerisation of the PBnMA block (DP_{PBnMA}) ranged from 500 to 1000, while the degree of polymerisation of the PS block (DP_{PS}) was kept at 400 for all three brushes studied (Tables 1 and 2). In

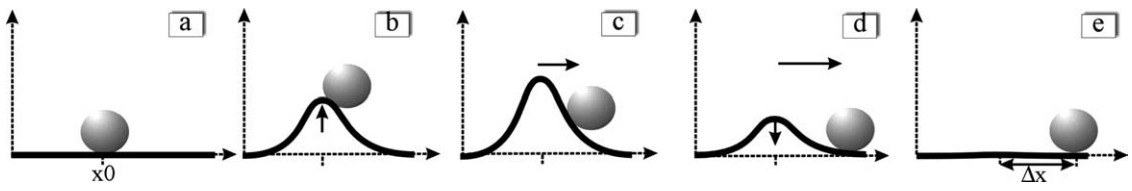

Fig. 3. Possible scheme of the action of a structural transition of a polymer brush on a nano-object adsorbed to its surface. The acting net force can be of diverse nature. When a structural element forms, the local, inhomogeneous chemical composition might attract or repel the object away from the element's center of mass. In this way, the nano object is subject to fluctuating force fields on a nano-scale during topography switching.

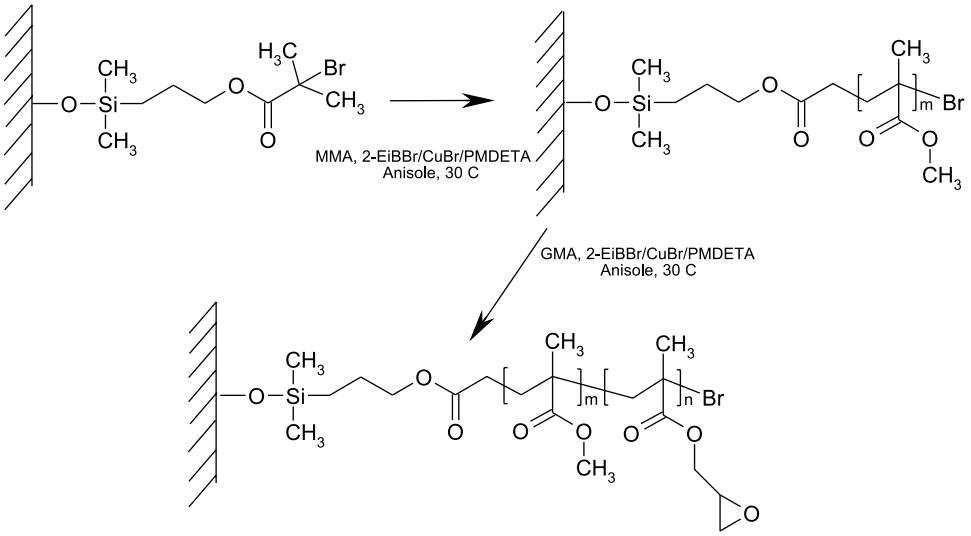

Scheme 1. Scheme of the synthesis of a p(MMA-*b*-GMA) diblock-copolymer brush.

the Tables 1 and 2 we list also the values of the dry thickness of the first layers of the brushes, as well as the total dry thickness of diblock-copolymer brushes measured by ellipsometry and X-ray reflectometry [48,49]. It is worth mentioning the ratio of the dry thickness of the first block to the dry thickness of the second block termed ϕ (Tables 1 and 2). Here height ratio is shown instead of mass ratio, as the difference of the density of the two polymers (PMMA and PGMA for the first brush, and PBnMA and PS for the second brush) is relatively small and the height ratio is an easily observable parameter.

Although the chemical structure of the two series of brushes differs, the samples were generated having similar ϕ values. It is 1.5 and 1.2 for brushes (a), 1.8 and 1.9 for brushes (b), and 2 and 2.6 for brushes (c) (Tables 1 and 2). Remarkably, the brushes of series (a), (b) and (c) show nanophase separation into similar patterns (Figs. 4 and 5). With increasing molecular weight of the first block (PMMA for the first series of brushes, and PBnMA for the second series), a transition between ripple-like (Figs. 4a and 5a) to worm-like (Figs. 4b and 5b), and to spherical-like patterns (Figs. 4c and 5c) was obsserved regardless of the chemical structure. The characterization of the surface topography was performed using an Atomic Force Microscope (Nanoscope IIIa, Digital Instruments). The microscope was operated in tapping mode, using commercial tips with a resonance frequency of ~300 kHz, and a spring constant of ~50 N/m. The AFM micrographs have been recorded in air at a temperature of around 23 °C [8].

Not only the general shape of the patterns of both brush series (p(MMA-*b*-GMA) and p(BnMA-*b*-S)) is correlated with each other, but also the size of the formed nano

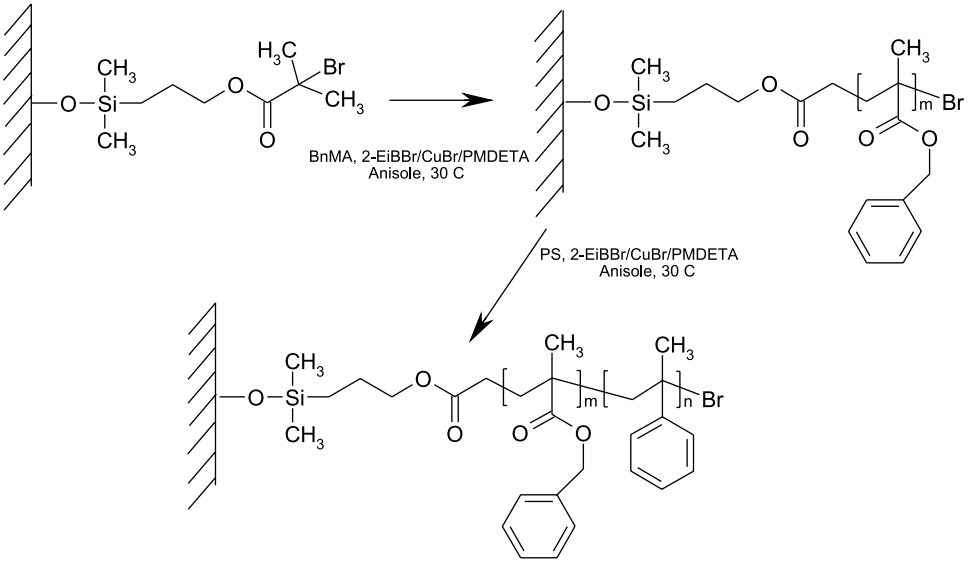

Scheme 2. Scheme of the synthesis of a p(BnMA-*b*-S) diblock-copolymer brush.

Table 1
Molecular characteristics of p(MMA-*b*-GMA) diblock-copolymer brushes [8]

	M_n^{PMMA} ($\times 10^3$ g/mol)	DP_{PMMA} [a]	M_n^{PGMA} ($\times 10^3$ g/mol)	DP_{PGMA}	h_{PMMA} [b] (nm)	h_{total} [c] (nm)	$\phi = h_{PMMA}/^{+}h_{PGMA}$ [d]
(a)	53	600	29	300	15	25	1.5
(b)	62	700	29	300	18	28	1.8
(c)	70	800	29	300	20	30	2

$^{+}h_{PGMA}$ is calculated as $h_{total} - h_{PMMA}$.
[a] DP was calculated as the ratio of M_n/M_0, where M_n is the number average molecular weight of the free polymers measured using an Agilent GPC setup, and M_0 is the molecular weight of the corresponding monomer unit.
[b] h_{PMMA} is the dry thickness of the first block measured by ellipsometry.
[c] h_{total} is the total dry thickness of the diblock-copolymer brush.
[d] h_{PGMA} is calculated as $h_{total} - h_{PMMA}$.

structures differs only slightly from one system to the other (Table 3).

As can be inferred from Table 3, the height of the features formed by the second brush series p(BnMA-*b*-S) decreases from 10 to 5 nm with increasing length of the first block (with the transition from ripple-like to spherical-like pattern), while the distance between two neighbouring elements increases from 40 to 50 nm. The size of the patterns of the first series of brushes p(MMA-*b*-GMA) is the same for all three patterns (Table 3).

Each pattern can be turned into a featureless, flat surface by exposing the sample to a good solvent for both blocks (Figs. 4d and 5d). The roughness of the flat surfaces, denoted by RMS (the root mean square deviation from the mean plane) is 0.4 nm for both types of diblock-copolymer brushes, similar to that of the homopolymers. In both cases, the good solvent is chloroform, while the selective solvent is toluene for the p(MMA-*b*-GMA) (good solvent for the PMMA block, poor solvent for the PGMA block), and acetone for the p(BnMA-*b*-S) (good solvent for the PBnMA block, poor solvent for the PS block). Re-exposing the brushes to a poor solvent (toluene or acetone) restores the structured topography. The transition is reversible over many periods of switching, checked for up to 100 times. The process of topography switching is rather quick: already 1 s of solvent exposition is enough for both series of brushes to turn the patterns into the flat state and back to the structured one. A more comprehensive discussion of the switching process is published elsewhere [8,50].

The distribution of blocks within the micelles and on the surfaces is not yet understood, as most spectroscopic techniques do not have the required nanometer resolution to analyse single domains, but average over larger surface area. Based on the results of contact angle measurements, for the flat state of the surface, one can assume that the second blocks PGMA and PS of both brushes build the top layer of the polymer surface (Table 4).

Table 4 shows that the advancing and receding contact angles measured on the flat surface of the p(MMA-*b*-GMA) brush are $\theta_a = 55°$, $\theta_r = 42°$, close to the values for the homopolymer brush PGMA ($\theta_a = 56°$, $\theta_r = 42°$). In the structured state (after treatment with toluene), we found $\theta_a = 65°$, $\theta_r = 50°$, which are values in between the ones for the homopolymer brushes PMMA ($\theta_a = 74°$, $\theta_r = 60°$) and PGMA. The same tendency was found for the second type of brush p(BnMA-*b*-S) (Table 4). Within one series of brushes, the shape of the nanopatterns does not influence the value of contact angles. They are the same for ripple-like, worm-like and spherical patterns as the height of the patterns is too small to cause roughness induced changes of the contact angles.

Mixed brushes. In contrast to the diblock-copolymer brushes, where a living polymerisation technique is needed, mixed brushes can be prepared using free radical chain polymerisation [46]. Here we discuss only one example of a series of mixed brushes studied in our group. A more detailed analysis of the special case of mixed brushes can be found elsewhere [8,46,47,50]. Although the mixed brush system consisting of PMMA-PGMA (Scheme 3) discussed in this paper has the same chemical composition as the diblock-copolymer brushes consisting of p(MMA-*b*-GMA), the size of the structures occurring due to the nanophase separation is much larger as compared to those of the diblock-copolymers.

In Fig. 6, a typical AFM micrograph of a mixed brush of PMMA-PGMA, recorded in the dry state, is shown. After

Table 2
Molecular characteristics of p(BnMA-*b*-S) diblock-copolymer brushes [49]

	M_n^{PBnMA} ($\times 10^3$ g/mol)	DP_{PBnMA}	M_n^{PS} ($\times 10^3$ g/mol)	DP_{PS}	h_{PBnMA} (nm)	h_{total} (nm)	$\phi = h_{PBnMA}/^{+}h_{PS}$ [a]
(a)	94	600	48	400	37	67	1.2
(b)	140	800	48	400	57	87	1.9
(c)	185	1000	48	400	79	109	2.6

[a] h_{PS} is calculated as $h_{total} - h_{PBnMA}$.

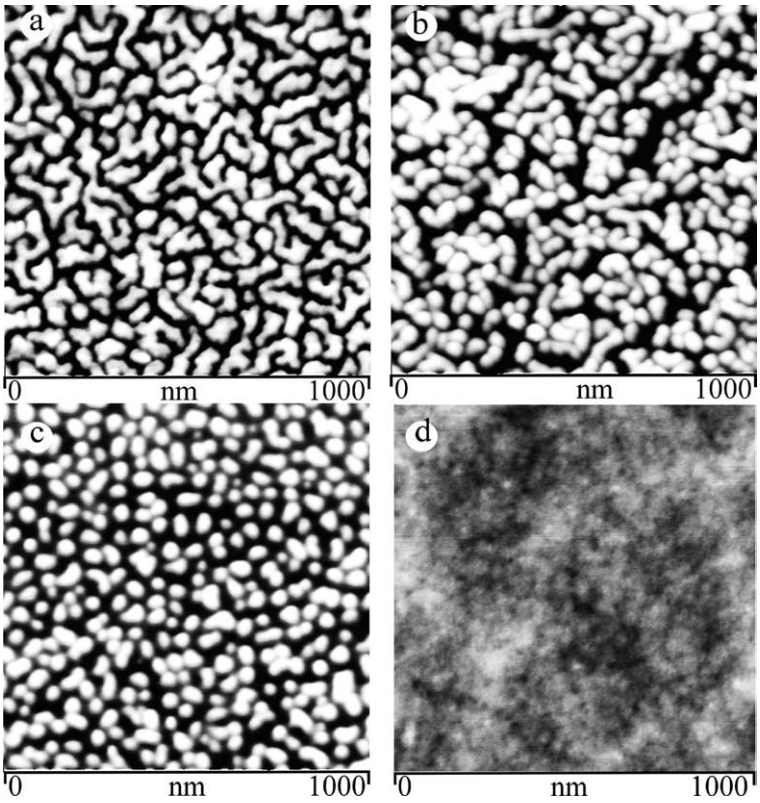

Fig. 4. AFM micrographs of p(MMA-*b*-GMA) diblock-copolymer brushes. Depending on the degree of polymerisation of the first attached PMMA block, the topography of the brushes appears as (a) ripple-like ($\phi = 1.5$), (b) worm-like ($\phi = 1.8$), and (c) spherical-like ($\phi = 2$). (d) The obtained structures can be turned into a flat, featureless surface by exposing the samples to chloroform, which is a good solvent for both blocks. The vertical scale for (a–c) is from 0 to 50 nm, while for (d) it is from 0 to 10 nm.

treatment with toluene (a poor solvent for PGMA), the brush shows nanophase separation to yield a 'crater-like' structure with 70–200 nm in diameter. The 'craters' have a depth of 20–70 nm (Fig. 6a), while the total film thickness as obtained with ellipsometry is 100 nm. The difference in the size of formed patterns between p(MMA-GMA) diblock-copolymers and PMMA-PGMA mixed brushes can be explained by the difference in molecular weight of the chains. The molecular weights of the PMMA and PGMA are 1.8×10^6 g/mol, and 2.4×10^6 g/mol, respectively [47], that is approximately one order of magnitude larger than in the case of diblock-copolymer brushes (Table 1). The patterns disappear after treating the sample with chloroform (a good solvent for both polymers) (Fig. 6b). As for the diblock-copolymer brushes, the transition is reversible over many cycles of topography switching. The advancing and receding contact angles measured on the flat surface of the brush are $\theta_a = 66°$, $\theta_r = 53°$, that is between the values for the homopolymer brushes PMMA and PGMA.

It should be emphasized here that the transitions described so far were observed ex-situ. That is, after recording the topography, the samples were removed from the AFM, exposed to a good or a poor solvent, dried in air for 15 min and then used re-examined with the AFM.

2.3.2. In-situ switching of the brush topography in vapors

For the in-situ investigation of the switching process, it is convenient to use solvent vapor instead of liquids. To perform the experiment, the solvent vapors have to be pumped directly into the area between the scanning AFM tip

Table 3
Size of nano patterns of p(MMA-*b*-GMA) and p(BnMA-*b*-S) diblock-copolymer brushes measured by AFM

	P(MMA-*b*-GMA)		P(BnMA-*b*-S)	
	H^a (nm)	D^b (nm)	H (nm)	D (nm)
a (Ripple-like)	10±1	50±5	10±2	40±5
b (Worm-like)	10±1	50±5	8±1	45±5
c (Spherical-like)	10±1	50±5	5±1	50±5

[a] H is the height of the patterns.
[b] D is the average distance between two neighbouring features.

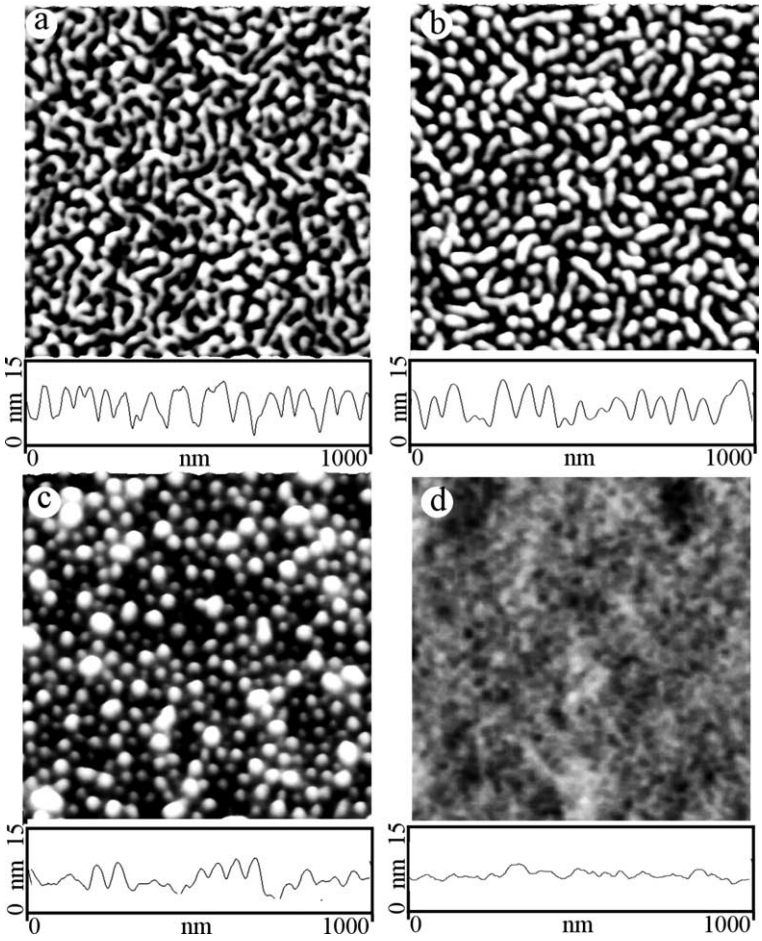

Fig. 5. AFM micrographs of p(BnMA-*b*-S) diblock-copolymer brushes. As in the case of the p(MMA-*b*-GMA) brushes (Fig. 4), the patterns differ depending on the length of the first block: (a) ripple-like ($\phi = 1.2$), (b) worm-like ($\phi = 1.9$), and (c) spherical-like ($\phi = 2.6$). (d) Flat, featureless surface is obtained after exposing the samples to chloroform. At the bottom of each AFM micrograph the corresponding cross-section of the micrographs is shown.

and the substrate. For this purpose, we have used an AFM liquid cell, connected to a specifically designed set-up, which allows it to periodically pump the different solvents and vapors through the cell. The details of the experiments are published elsewhere [50]. In Fig. 7, the in situ switching of the topography of the p(MMA-*b*-GMA) diblock-copolymer brush is shown, proceeding from the structured to the flat and then back to the structured state. After scanning the patterned substrate in air (Fig. 7a), chloroform vapor was pumped into the liquid cell at a point when the AFM tip was scanned from bottom to top (bold arrow, Fig. 7b). After a short signal instability induced by the vapor flow, corresponding to the area between the bold and the dashed arrows (Fig. 7b), the AFM image shows that the structure of the brush turned into the flat state. Thereafter we scanned the remaining area (Fig. 7b). At the beginning of the subsequent scan, toluene vapor was pumped through the cell (bold and dashed arrows on Fig. 7c). Although the change in topography is not pronounced, a closer inspection (inset in Fig. 7c) shows that a very similar topology as compared to the starting point in Fig. 7a occurred. The distance between two neighbouring features is again 50 nm, whereas the height of the patterns is not completely restored, and is only 5 nm. Only after a longer period of pumping

Table 4
Advancing and receding contact angles (against water) on structured and flat surfaces of p(MMA-*b*-GMA) and p(BnMA-*b*-S) brushes

	P(MMA-*b*-GMA)		P(BnMA-*b*-S)	
	θ_a (deg)	θ_r (deg)	θ_a (deg)	θ_r (deg)
Structured state	65	50	85	73
Flat state	55	42	95	83

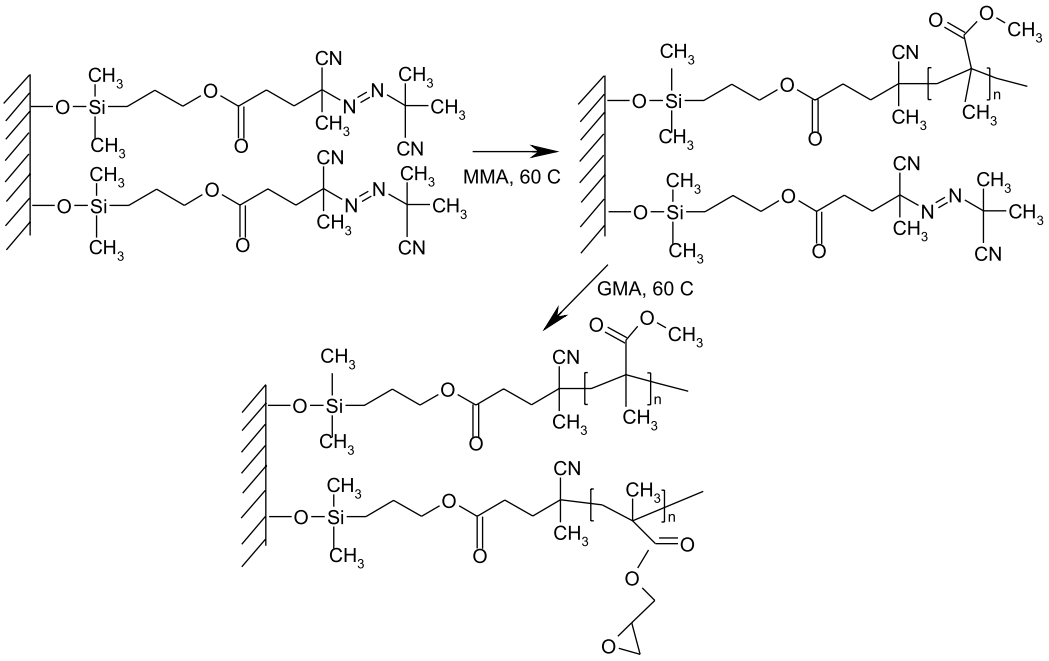

Scheme 3. Scheme of the synthesis of a PMMA-PGMA mixed brush.

toluene vapor (∼1 h) through the cell, the original height of the structure is restored and the micrograph can no longer be distinguished from that shown in Fig. 7a.

The vapor induced transition is reversible over many switching cycles. The only difference to the solvent induced transition is that the recovery of the original structure, when exposed to vapor, takes longer. Since chloroform is a good solvent for both blocks, it takes comparably longer to replace it with toluene vapor, which is only a good solvent for the first block. An upper estimate for the time needed for topography switching in vapor can be inferred from the in-situ experiment, by looking at the instability period of the continuous AFM image recording in Fig. 7. It lasts for roughly 13 s, the actual switching of course, may be faster.

A very similar behavior of the in-situ transition from the structured to the flat state of the topography was found for the p(BnMA-*b*-S) diblock-copolymer brushes. In Fig. 8 the identical experiment described above is shown.

The same behavior was found for worm- and spherical-like pattern. These results are presented in Fig. 9.

In the case of mixed brushes, an in-situ experiment was done using the very same protocol (Fig. 10). Here, the instability induced by the flow of vapor is not so pronounced as in the case of the diblock copolymer brush (Fig. 10b), but the transition appears to be slower. Thus, in the case of diblock-copolymer brushes, the time between the injection of vapor and the transition is 13 s, while for the mixed brush 20 s are needed. The recovery of the patterns of the mixed brush is not as complete as in the case of the

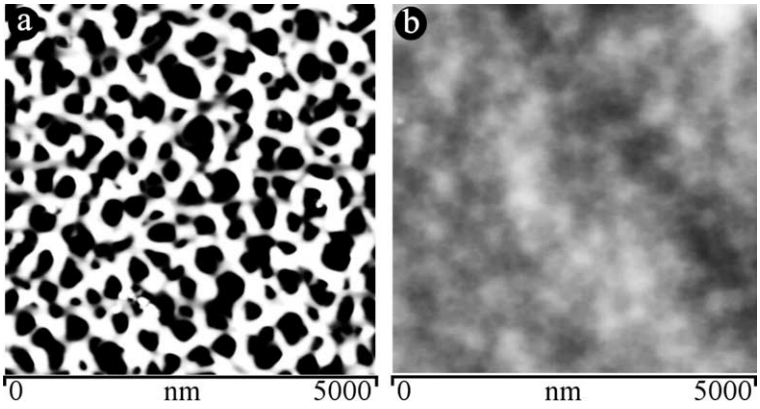

Fig. 6. AFM micrographs of a mixed brush consisting of PMMA and PGMA chains. (a) After treating the sample with toluene, the brush shows nanophase separation with a ‘crater-like’ structure. (b) Treating of the sample with chloroform causes vanishing of the structured topography. The surface is featureless and its RMS roughness is 0.8 nm.

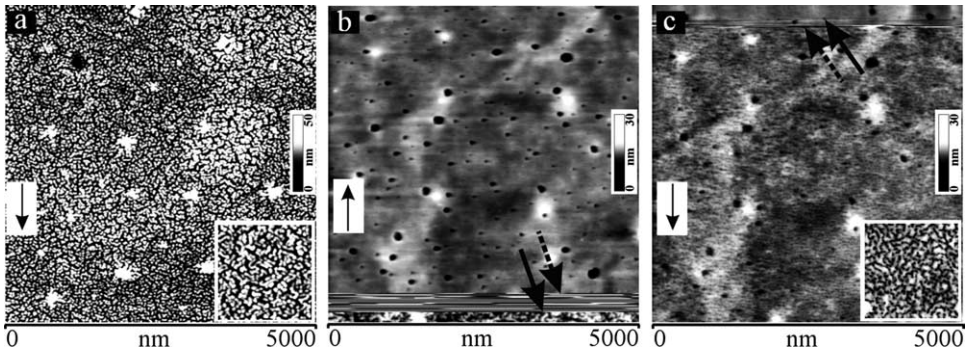

Fig. 7. AFM micrographs of the in-situ switching of the topography of a p(MMA-*b*-GMA) diblock-copolymer brush. (a) Image of the structured state of the brush, scanned in air from top to bottom (the direction of the scanning is pointed out by the arrow). (b) At the beginning of the subsequent scan, chloroform vapor was pumped into the area between brush and tip at the position indicated by the bold arrow. After a certain time of instability during which the tip travelled a distance of 280 nm (start marked by a bold, end position marked by a dashed arrow), the structure of the brush turned into a featureless, flat topography. (c) At the position marked by the bold arrow, toluene vapor is pumped through the system. The instability region in this case is smaller (110 nm). Upon exposure to the toluene vapor, the brush is found to nanophase separate again. Micrographs inserted in a, and c show magnifications of regions with area 1 μm × 1 μm, depicting the structure of the polymer surface more clearly [8]. The *z*-scale is inserted into each micrograph.

diblock-copolymer brush. Moreover, the mixed brush in the flat state, after treatment with chloroform vapor, exhibits a higher RMS value in comparison to the case of treating it with the solvent. This might be due to the fact that the swelling of the thick mixed brush is not complete during a short period of exposure to chloroform vapor (4 min and 20 s).

Summarizing the results on the structure changes of different brush compositions, we have demonstrated how to control the reversible transitions of diblock-copolymer and mixed brushes between a nano structured and a flat topography. Moreover, we have shown that the transition can be induced by vapor instead of liquid solvent. This opens up the possibility to monitor this process in-situ, when, during scanning, the vapors are pumped through the liquid cell and are periodically exchanged. The transitions of the structures in vapor require more exposition time than in liquid. When comparing to the structures after the changes in liquid, we also find a recovery of the original pattern, but not quite as complete, when a similar time frame is chosen. This is due to the fact that the good solvent for both blocks could not completely be replaced by the poor solvent for the second block in the given timeframe.

2.3.3. Domain memory

In this section we discuss whether the brush locally forms the same pattern every time the transition to the structured state occurs, or if the local assembly of the domains (ripples, worms, spheres) emerges in different places each cycle of switching. This is especially relevant for understanding the nature of the motion process as discussed in the next section. In general, this question has not been addressed so far. An exception is the study of the formation of nematic domains in so-called LC-brushes (polymer brushes with liquid crystalline side chains), where a strong memory effect between the location of LC-domains before and after erasing of the structure and return to the LC-phase was found [51]. However, the mechanism of domain formation

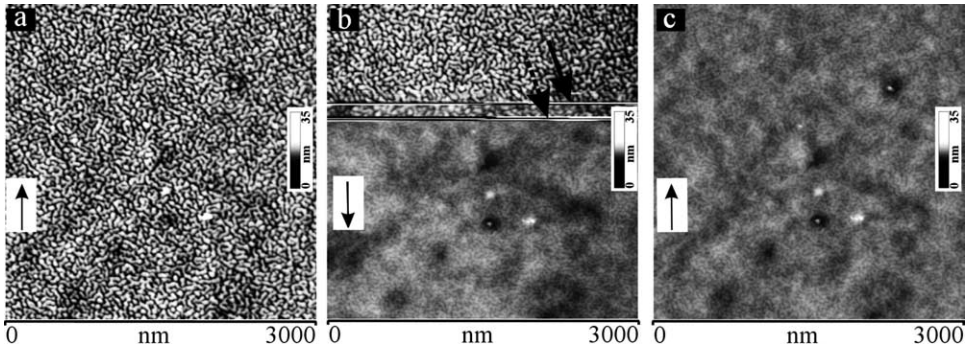

Fig. 8. AFM micrographs of the in-situ switching of the topography of a p(BnMA-*b*-S) diblock-copolymer brush, here from a ripple-like pattern ($\phi = 1.2$) to the flat state by chloroform vapor. (a) Image of the pattern state of the brush, scanned in air with the scanning direction from bottom to top (marked by an arrow). (b) During scanning from top to bottom at the point marked by the bold arrow, chloroform vapor was pumped into the liquid cell. After a short time of instability, the image revealed a transition to a flat topography. (c) Subsequent scanning of the same area shows a flat, featureless topography of the brush with a roughness of RMS = 0.4 nm.

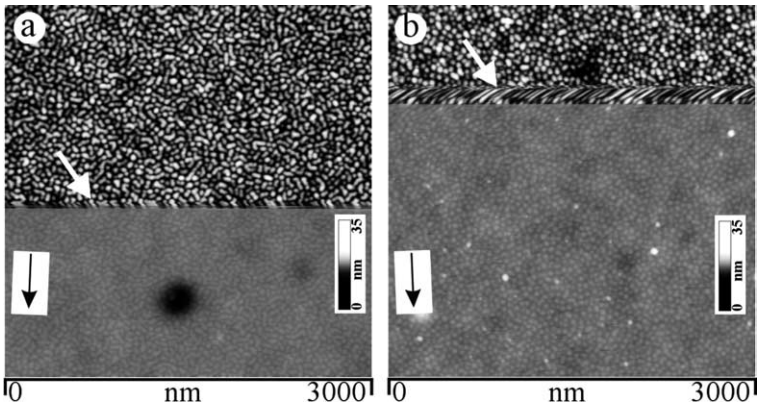

Fig. 9. AFM micrographs of the topography switching of the p(BnMA-*b*-S) diblock-copolymer brushes. The patterns of the brushes disappeared after pumping chloroform into the area between the brush surface and the scanning AFM tip. (a) Brush showing a worm-like pattern ($\phi = 1.9$), (b) brush showing a spherical pattern ($\phi = 2.6$).

in LC-brushes is different compared to that in diblock-copolymer and mixed brushes, and will further be discussed in a more detail in forthcoming publication [52]. Here, we will only briefly report some aspects of this work.

Investigations of domain memory effects require a reliable point of reference on the brush. For an experiment with a p(BnMA-*b*-S) diblock-copolymer brush we chose a location showing certain characteristic defects that could easily be identified (Fig. 11a–c). There are three sites of depression of the brush height that are found close to an edge of the sample. The general proceeding is as follows. First, the brush structure just after synthesis was imaged (Fig. 11a), and a specific area close to the reference sites was selected for successive magnification (Figs. a1 and a2). Then the brush was treated with chloroform solvent, turning the topography into the flat state. Even then the defects are clearly visible (Fig. 11b). This allows for a safe identification of the area chosen after subsequent treatment with acetone solvent, when the brush turns back into the ripple-like structure (Fig. 11c). The magnification process (Fig. c1 and c2) reveals that for the diblock-copolymer brush used in this example there is no obvious correlation between the location of domains before and after solvent treatment. The same behavior can be also observed for the other type of p(MMA-*b*-GMA) diblock copolymer brushes. Of course, it cannot be ruled out that there is still some residual correlation across several successive patterns. Although this point could be of interest for a theoretical description of such systems, it must be left to a quantitative analysis that is being carried out currently.

Repeating the same analysis for a PMMA-PGMA mixed brush reveals a completely different situation (Fig. 12). Here, the area of reference was identified according to the positions of 100 nm silica particles adsorbed on top of the brush (bright spots in the micrograph). After one cycle (Figs. 12a and a1) and 5 cycles (Figs. 12b and b1) of switching, the AFM micrographs appear as almost identical. The size, shape, and location of individual domains is 'remembered' by the brush, even though it was for an extended period of time in a flat, featureless state ('surface

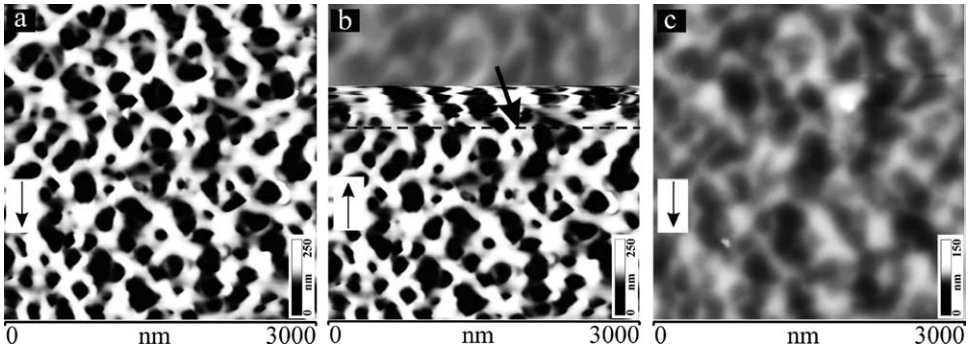

Fig. 10. AFM micrographs of the in-situ switching of the topography of a mixed brush. (a) The PMMA-PGMA brush shows nanophase separation after treatment with toluene. The scanning direction is from top to bottom (indicated by an arrow). (b) During scanning from bottom to top, chloroform vapor is pumped into the liquid cell when an AFM tip reaches the position marked by the dashed line (bold arrow). After a certain period at which the distance of 415 nm is scanned, the 'crater-like' structure disappeared. (c) Subsequent scanning of the same area of the brush. The brush shows a smooth topography. The *z*-scale is shown for each micrograph.

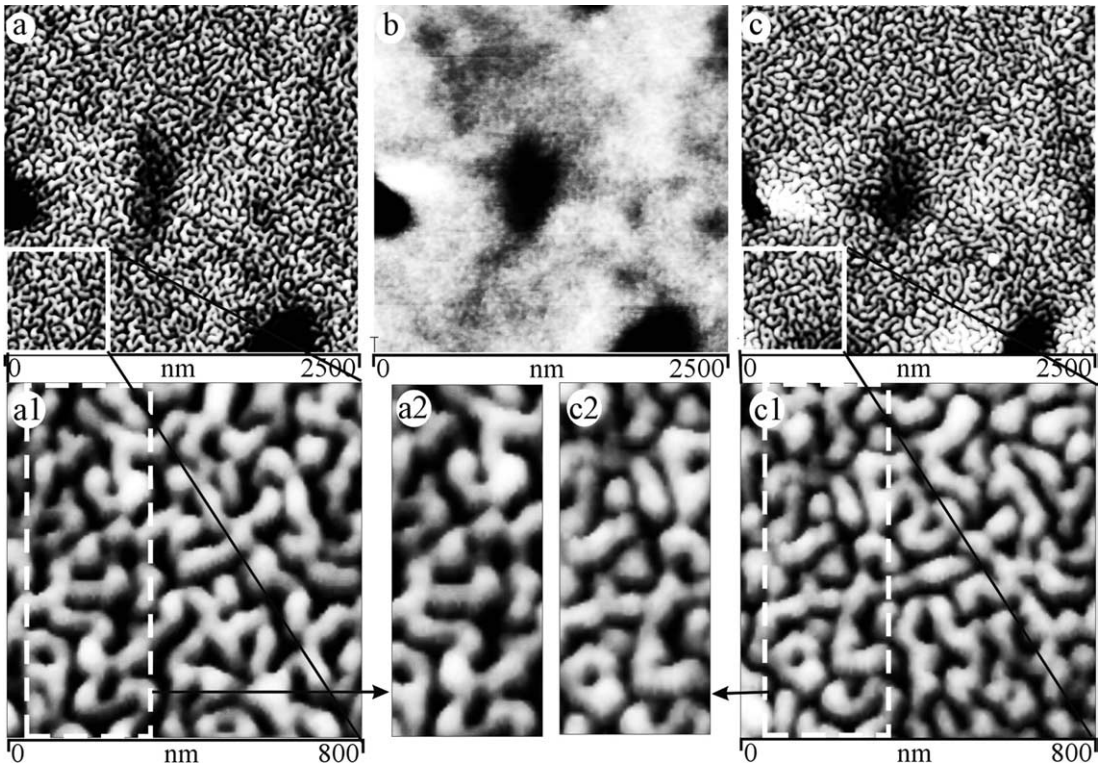

Fig. 11. AFM micrographs of a p(BnMA-*b*-S) diblock-copolymer brush recorded in air: (a) just after preparation, (b) after exposure to chloroform for 1 min, (c) after subsequent exposure to acetone for 1 min. In figure (a) and (c), a white square signifies a reference area magnifications of which are shown below (Figs. a1–a2 and c1–c2).

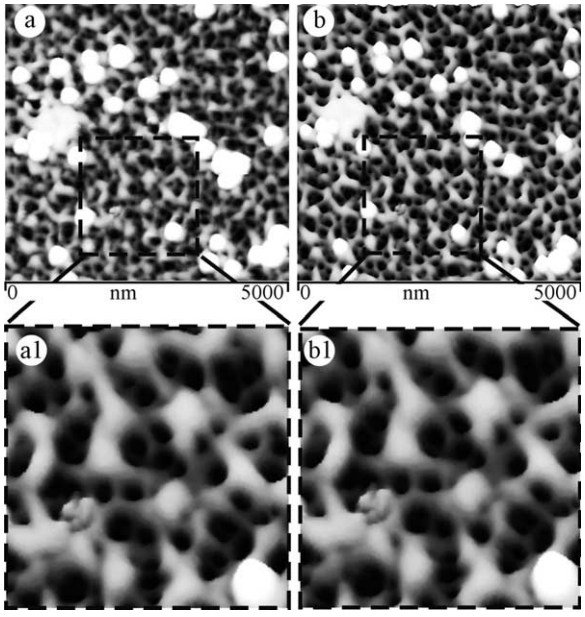

Fig. 12. AFM micrographs of a mixed brush: (a) before the switching procedure, (b) after five cycles of topography switching. (a1) Enhancement of the selected area in Fig. 12a is marked by a dashed black square, (b1) enhancement of the same area (marked in Fig. 12b by a black dashed square) after 5 cycles of topography switching. In both micrographs, a nano sphere in the lower right corner of the area can be used as a point of reference.

memory effect'). This remains valid qualitatively even after several cycles of switching; here it was checked for up to 20 cycles.

To summarize, the diblock-copolymer brushes do not exhibit a domain memory effect. The formed features (ripples, worms, spheres) have the same characteristic size (height, and the average distance between two neighbouring elements), but appear randomly within the brush each time after topography switching, i.e. there is no correlation between the position of a domain before and after flattening and restoring of the nano structure. In contrast, the mixed brush system has a strong domain memory effect, i.e. the domains appear always on the same location after each cycle of topography switching. The reason for this strong difference of the behavior of two seemingly rather similar systems is not yet understood and requires further investigations.

2.4. Organization of silica nano spheres on diblock-copolymer and mixed brushes

2.4.1. Motion of nano spheres due to topography switching of diblock-copolymer brushes induced by solvent treatment

Having understood how to control the transition of the topography of diblock-copolymers and mixed brushes between the two states, patterned and flat, we have studied whether these transitions can cause a movement of nano spheres adsorbed on top of the surfaces. As nano objects we choose silica particles of 50 nm in diameter, which closely corresponds to the average distance between two neighboring structure elements of the diblock-copolymer structures. The silica particles were synthesized in our laboratory using a slight variation of Stöber's original process [53]. The surface of the spheres is covered by OH groups (5–6 OH-groups per nm^2), that render the particles hydrophilic.

The silica particles were adsorbed on top of diblock-copolymer brushes by spin casting at 2000 rpm from ethanol solution with a concentration of 1 wt%. Just after adsorption, the silica particles do not form aggregates, and are situated randomly on the structured polymer surface (Fig. 13a). In Fig. 13a, one can also see very clearly the underlying structured surface of the diblock-copolymer brush (same brush in Fig. 4b with the worm-like structure, $\phi = 1.8$). This indicates that the brief contact of the ethanol solution with the brushes does not alter the topography of the brush. After recording the AFM micrograph, we removed the sample from the microscope and placed it for 10 s in a good solvent for both blocks (chloroform). Then we dried the sample in air for 15 min and recorded the distribution of the silica particles. Fig. 13b shows groups of two or three silica particles forming islands on the flat featureless surface of the underlying brush. During restoration of the patterned brush structure upon exposure to toluene (poor solvent for the second block) even further aggregation was observed.

Iterating over more cycles, the formation of large elongated aggregates occurs (Fig. 14). The total number of the adsorbed silica spheres remains the same over many switching cycles, i.e. desorption does not take place. The height of the particles is recorded to stay constant at 50 nm, indicating that particles do not sink into the polymer layer [8].

The experiments on silica particles were conducted ex-situ, thus it was not possible to stay on a specific spot on the brush. It was checked however, that the particle distribution was sufficiently homogeneous across the whole substrate, so that different areas are indeed equivalent. To characterize the distribution of the single spheres during the switching process, in Fig. 15 we plot the number of single silica spheres on a 10 μm × 10 μm area as a function of the switching cycles.

Just after adsorption of silica particles, they are found as single specimens (relative number of isolated spheres is 100%). With increasing number of switching cycles, the number of isolated particles decreases, until it settles to a plateau of roughly 20% after 8 cycles and remains constant thereafter. This, however, does not imply a stationary state, the size of some fraction of the islands still grows, while the percentage of single spheres remains 20%. The explanation for this seemingly contradictory finding is, that particles at the periphery of the islands can leave them and become isolated again, or join different islands.

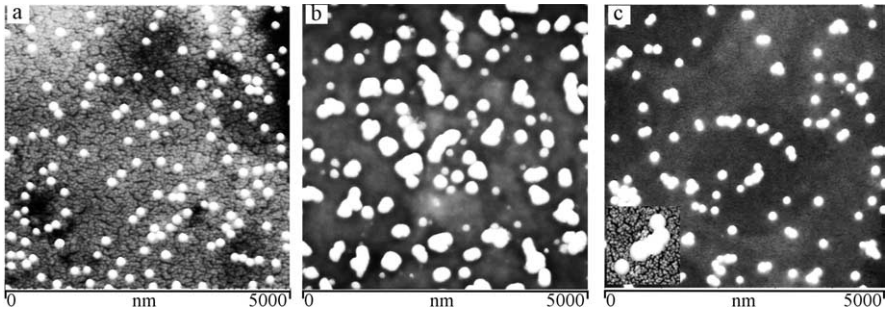

Fig. 13. AFM micrographs of silica spheres adsorbed on top of a diblock-copolymer brush. (a) After adsorption, the spheres were found as single specimens situated randomly on the structured surface. (b) After switching the topography into a flat, featureless state by exposing the sample to chloroform for 10 s, the spheres form aggregates consisting of two and three particles. (c) Recovering the structured state (treatment with toluene during 10 s), results in further aggregation of spheres. The inserted picture shows details of the underlying surface.

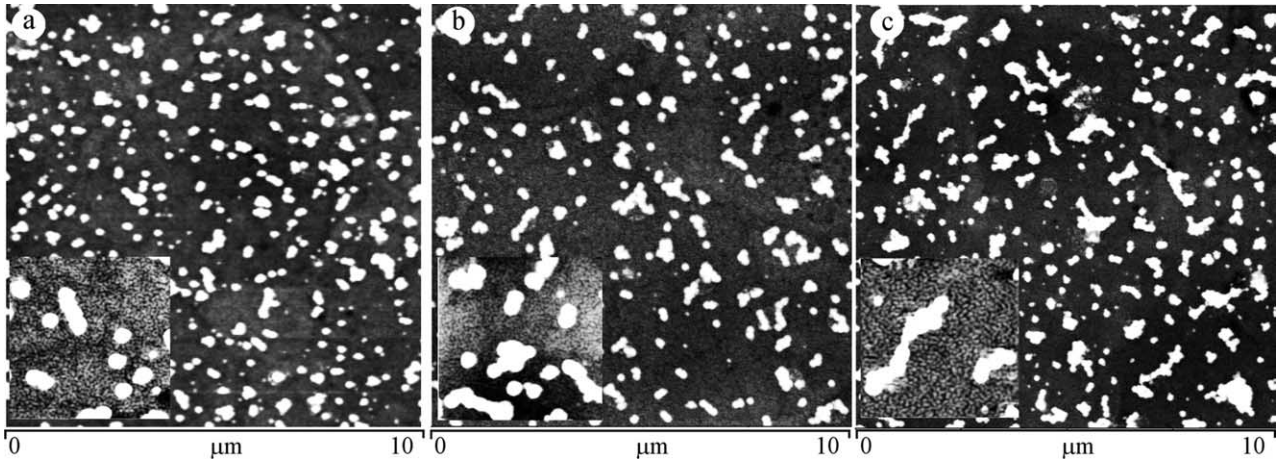

Fig. 14. The AFM micrographs in (a) and (b) show the particle distribution after 5 and 10 cycles, respectively. The spheres become increasingly aggregated. (c) After 26 cycles, the formation of elongated islands of silica nanoparticles was observed. Micrographs inserted in a, b, and c show magnifications of regions with area 2 μm×2 μm, depicting more clearly the underlying structure of the polymer carpet.

For all three kinds of brushes shown in Fig. 4 (ripples, worms and spheres), the process of particle motion and aggregation appears to be almost identical. Only on the brush with the shortest first PMMA-block (ripple-like structure, Fig. 16a), elongation of islands is found to be particularly pronounced, and can be best described by the formation of strings of silica particles (Fig. 16b). This indicates that details of the brush pattern and of the transition between different patterns does indeed have an influence on particle motion and aggregation.

On p(BnMA-*b*-S) diblock-copolymer brushes, the silica nanospheres were washed off the surface during the solvent treatment. The switching of the brush topography in vapor, where no capillary forces act on the nano spheres, lead to the same motion of nano spheres as described above for the case of p(MMA-*b*-GMA) brushes [52].

To check whether aggregation appeared because of pattern switching or on account of other reasons, we have carried out the very same experiments with homopolymer brushes of PMMA and PGMA, with molecular weight and grafting density similar to the diblock-copolymer brush (0.25 chains/nm^2 [8]). In the case of homopolymer brushes, no aggregation of the nanoparticles was found (Fig. 17). Additional annealing in a good solvent (chloroform) at room temperature during 24 h does not lead to changes in particle distribution.

It clearly indicates that only the switching process is responsible for the motion of nano particles, simple diffusion can safely be neglected (for more details see Section 3).

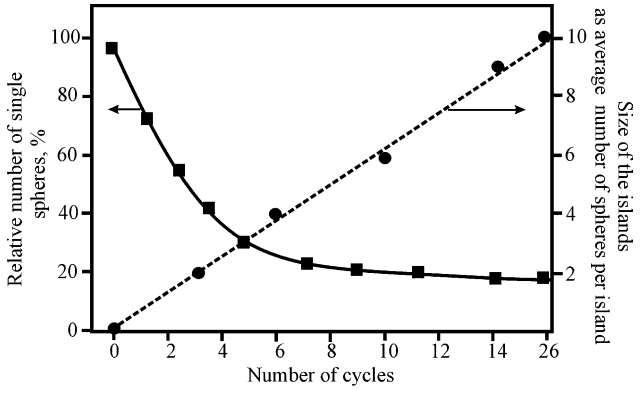

Fig. 15. Relative number of single silica particles, calculated as ($N_{single}/N_{total}\times100\%$), and the size of the islands over the number of switching cycles.

2.4.2. Organization of nano spheres on a mixed brush

Repeating the very same experiment with mixed brushes which form crater-like structures, we have found that the particle respond in a very different way. In contrast to diblock-copolymer brushes, the particles did not gather, but were simply 'swallowed' by a crater element. This can be inferred from an apparent decrease of particle height. When measured just after adsorption a value of 50 nm was obtained, while after the switching procedure the height decreased to 20 nm (Fig. 18b). As the silica particles do not shrink during solvent exposure, the height decrease is due to the particles sinking into the brush. In Fig. 18, particles are shown that are adsorbed on a flat substrate of a mixed brush. Before adsorption, the topography was rendered flat with chloroform, in order to prevent a gathering of silica particles in craters prior to the actual switching procedure.

This clearly shows that the motion of objects on a structured polymer surface is in general very sensitive to the length scales of patterns as compared to particle size. Currently, we are working on experiments with particles of diameter 200 nm. It is to be expected that they show the same behavior as the smaller silica particles on smaller structures; however, it is not known if the size of formed islands scales with the number of iterations in the same way. One would expect that since surface energy scales as

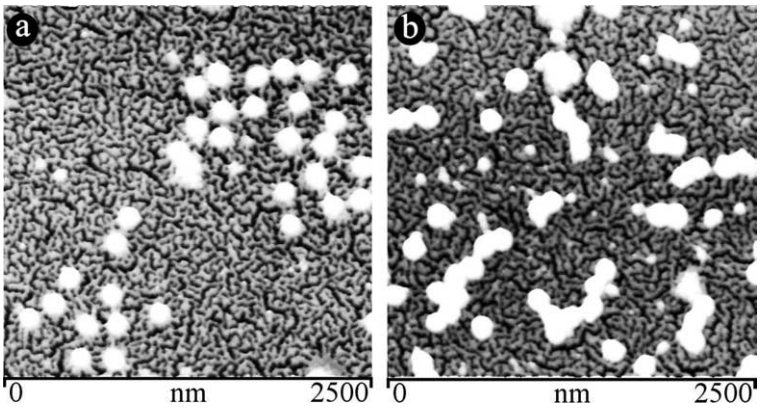

Fig. 16. AFM micrographs of silica particles adsorbed on top of a p(MMA-*b*-GMA) diblock-copolymer brush with a ripple like structure (shortest PMMA-block). (a) Silica particles are well separated just after adsorption. (b) After 20 cycles of switching the silica particles form elongated islands that can best be described as strings. On both micrographs one can clearly see the underlying ripple-like structure of the brush.

diameter squared, but the particle mass as diameter cubed, it might take a longer time for islands to form.

2.4.3. Motion of nano spheres due to topography switching of diblock-copolymer brushes induced by vapor treatment

The previous results were all obtained with the solvents chloroform and toluene. In this section, we want to give a brief summary of the analogous experiments conducted with solvent vapors, where recovering the structured brush states appears to be less complete. To check whether an incomplete transition is sufficient to initiate the process of motion, we have investigated the organization of nanoparticles on diblock-copolymer brushes similar to the case of ex situ switching (Fig. 19). This study was also performed with silica nanoparticles with 50 nm in diameter, which is larger than the average thickness of the brush (30 nm), but corresponds to the characteristic length scale of a pattern. It was found that as in the case already reported, just after adsorption from proper solution, silica nanoparticles showed no aggregation, and are situated as single specimens on the top of the ordered polymer surface (Fig. 19a). Thereafter, we performed in vapor ex-situ switching of the structure from patterned to featureless and back, when the substrate was first exposed to chloroform vapor and then to toluene vapor. As in the case of solvent treatment, already after the first cycle of switching, the formation of small clusters of nanoparticles was observed (Fig. 19b). Reiterating over more cycles, the formation of big elongated aggregates occurred (Fig. 19c) as well.

3. Suggested mechanism of motion

Wrapping up the previous findings, one might ask what the nature of the physical process of motion of the nano particles is.

Before dwelling on our proposed transport mechanism, we should first take other sources into consideration that could make nano particles move, namely, aggregation induced by diffusion and capillary forces acting on particles during solvent switching. These two reasons, however, can be ruled out for the following reasons: (i) the experiments

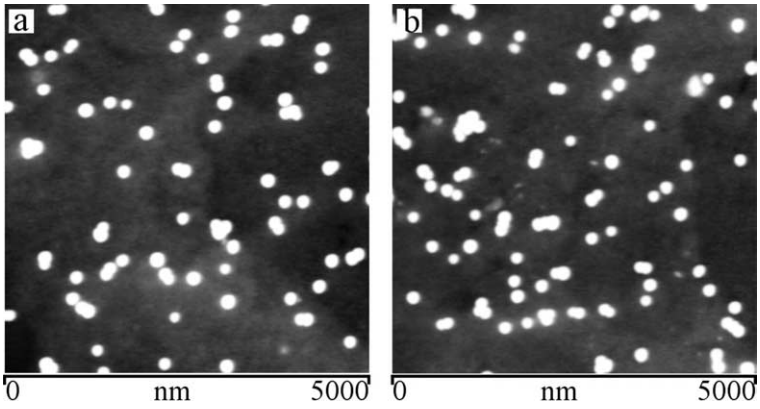

Fig. 17. AFM micrographs of silica nanoparticles adsorbed on a PGMA brush of 30 nm thickness: (a) just after adsorption, (b) after 26 switching cycles (chloroform/toluene) and annealing in good solvent during 24 h. In contrast to the diblock-copolymer brush (see Fig. 14), no aggregation of the nanoparticles was found.

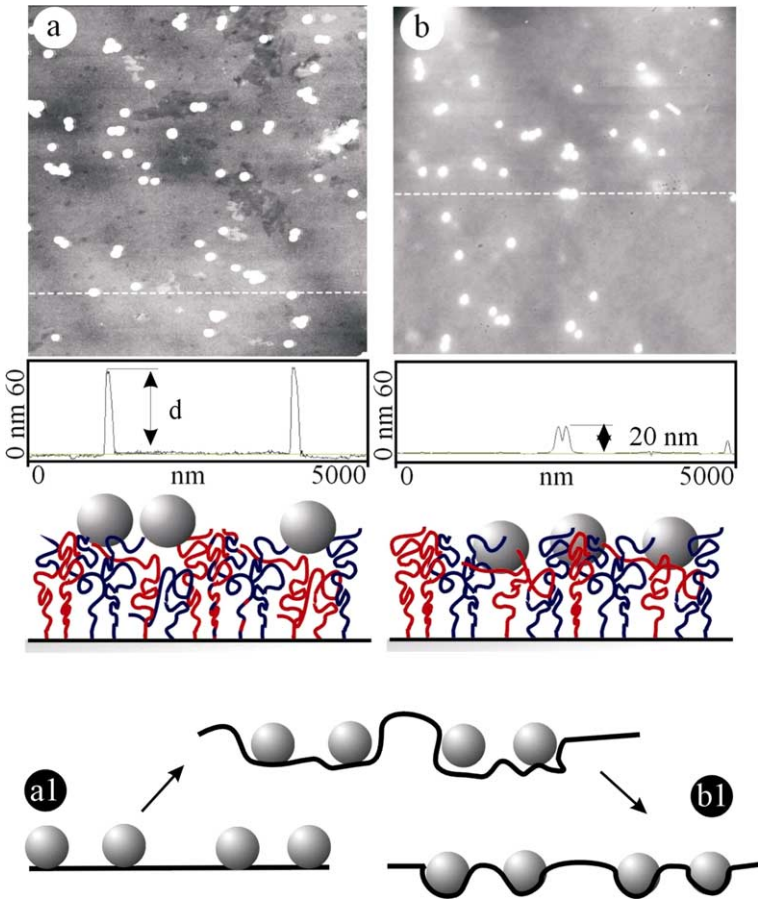

Fig. 18. AFM micrographs of silica particles adsorbed on a carpet made from a mixed polymer brush. (a) Just after adsorption on a flat surface of the brush, and (b) after 10 cycles of topography switching. The dashed lines indicate the tracks along which the cross section of the silica particles was recorded, as depicted below. A schematic view of the particles of how they situate on top of the carpet is also shown (a1 and b1).

with homopolymer brushes show clearly that silica particles do not aggregate when undergoing the very same procedure that was used for diblock-copolymer and mixed brushes: cyclic treatment with the solvents chloroform and toluene, and additional annealing in chloroform for 24 h; (ii) the experiments performed in vapor, where no capillary forces are present, yield results equivalent to those with solvent. Moreover, the statistical analysis of the number of single silica particles over number of switching cycles (compare Fig. 15) sustains this view. One can conclude that despite aggregation of nanospheres, there is an active exchange of particles between islands. This finally puts strong evidence

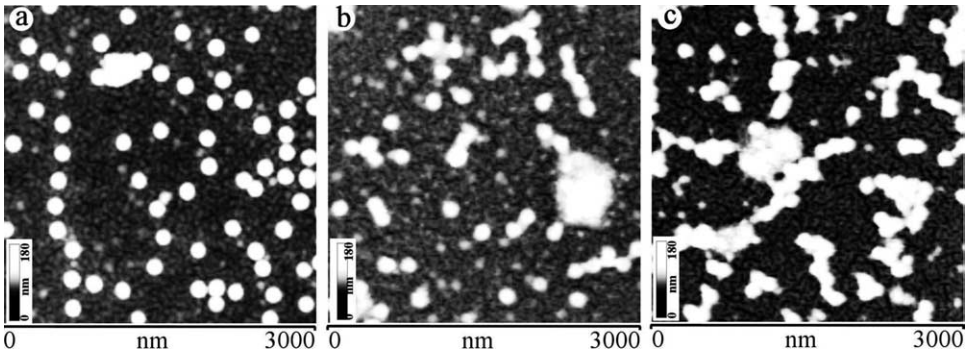

Fig. 19. AFM micrographs of the organization process of silica nanoparticles on a p(MMA-*b*-GMA) diblock-copolymer brush. (a) Nanoparticles adsorbed from ethanol solution formed no aggregates on the nanophase separated brush; (b) after exposition of the substrate to chloroform and then to toluene vapor, partial restoring of the pattern structure of the brush takes place. Some of the particles have started to form islands consisting of two, three or sometimes five objects. (b) Further aggregation into islands of the nanoparticles was observed after treating the substrate repetitively over several periods (50 cycles).

Table 5
Estimation of forces acting on a nanoparticle with 25 nm radius [54]

Gravity 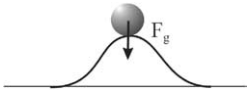	$F_g = mg = (4/3)\pi r^3 \rho g$; $\rho \approx 1$ g/cm^3, $r = 25$ nm, $g = 9.8$ m/sec^2	$F_g \approx 10^{-9}$ nN
Van der Waals Forces 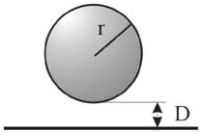	$F_{vdW} = Ar/6D^2$; $A = 10^{-19}$ J, $D = 0.3$ nm, $r = 25$ nm	$F_{vdW} \sim 5$ nN
Adhesion 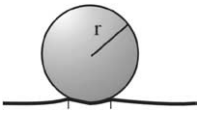	$F_{adh} = 4\pi r\gamma$; $\gamma = 2(\gamma_s\gamma_p)^{1/2}$, $\gamma_s = 100$ mJ/m^2 silica surface energy $\gamma_p = 25$ mJ/m^2 polymer surface energy	$F_{adh} \sim 30$ nN
Interparticle interactions 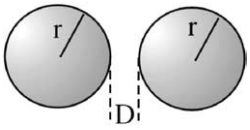	$F_{vdW} = Ar/12D^2$; $F_{adh} = 2\pi r\gamma_s$, $A = 10^{-19}$ J, $D = 0.3$ nm, $r = 25$ nm	$F_{vdW} \sim 2$ nN, $F_{adh} \sim 15$ nN

on the topography change as the only mechanism of colloid motion.

After having excluded such 'trivial' mechanisms, we now come back to a point of view already worked out in the introduction. Along with topographical changes due to nanophase separation, there is a profound and distinct change of associated surface energy on roughly the same length scale as the colloid size. Although we do not have a precise theoretical model of the motion process, we are now in the position to lay down some heuristic outline on how the development of a suitable theory might proceed.

As already mentioned, one can first rule out any gravitational component; van der Waals and adhesion forces are many orders of magnitude larger (Table 5). When the object's size is of the order of or slightly larger than the brush structure elements, a simple picture using the surface energy of the contact area between colloid and structure elements seems reasonable. For now, with the surface energy we formally include different kinds of forces which might contribute to the net force on the adsorbed colloid. It should be noted that here very simple models are used and the interaction values obtained can be only used to give an estimation of the order of magnitude of the forces involved.

The forces are calculated for the simple case of solid, non deformable surfaces in vacuum. A is the Hamaker constant, a typical value being 10^{-19} J. The value of $\gamma_p = 25$ mJ/m^2 is chosen as a typical surface energy for polymer surface.

When topography switching occurs, the area of the surface patches of structure elements in contact with or in the vicinity of the nano object changes, resulting in dynamically competing surface forces acting on the particle, as illustrated in Fig. 20. Repeating this process over many

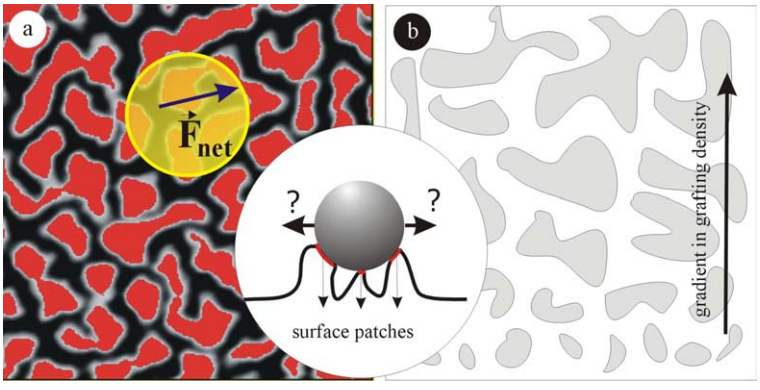

Fig. 20. The central picture shows how during an elementary step of motion its direction is determined: (a) vanishing and emerging adherent surface patches compete with attracting an adsorbed colloid. (b) Applying this picture, directed motion might be imposed by a gradient in the average area those surface patches assume. This can be achieved, e.g. by a gradient in grafting density or molecular weight of the attached polymer chains.

cycles, one can think of a dynamically fluctuating force field that, in general, would result in random motion of the nanospheres. In some respect this motion is similar to Brownian motion, but with elementary steps coupled to the switching process that in turn is imposed by the experimentalist.

More information will certainly be obtained when in-situ experiments are carried out in which the motion of a single particle is tracked. These experiments are going to be performed in vapor.

4. Conclusions and outlook

In this paper, we have reviewed a new approach to move nano objects on a surface made from polymer brushes. We have shown that structural changes of a diblock-copolymer brush during nanophase separation can be used to drive appropriately sized nano particles across the surface. Here, we have discussed this for certain types of p(MMA-*b*-GMA) and p(BnMA-*b*-S) diblock-copolymer brushes. As a starting point, we analysed the nanophase separation behavior of the brushes. Depending on the length of the first block (PMMA for the first series of brushes, and a pBnMA block for the second series of brushes) different shapes of patterns are formed, such as ripple-like, worm-like, and spherical. The mixed brush shows also nanophase separation in selective solvent into a 'crater'-like pattern, but the characteristic size of the pattern is much larger than in the case of diblock-copolymer brushes.

The patterns can be switched into a flat, featureless state by exposing them to a good solvent for both blocks. We have also proven that the transitions are reversible for more than 100 cycles. Furthermore, it was shown that vapor is already sufficient to induce the phase transitions, although the recovery of the surface pattern takes a longer time than in the case of solvents. This, however, does not seem to affect the efficiency of driving the colloid. The experiments suggest that in the vapour case one might need only a few additional cycles of switching in order for the particle to travel a comparable distance.

Returning to the very process of nano particle motion, up to the present we have shown that the periodical switching of the underlying topography indeed induces motion of nano objects, that eventually leads to formation of larger aggregates. On account of our experimental results, we have outlined a scheme of how a corresponding theory of colloid motion might be developed. More experimental light will be shed on this question when tracking the motion of a single particle during in situ pattern switching of the supporting polymer brush. The experiments with vapors represent an important prerequisite for this.

With respect to establishing a new mechanism for actually transporting objects in some predefined direction, our work reported here is only a first step. Several issues still need to be clarified, such as more details of the motion process.

A precise understanding of this will guide us in tailoring the pattern formation of diblock copolymer brushes, which has not been investigated until now, theoretically as well as experimentally. For instance, in order to determine a net direction of motion, a certain correlation of patterns between subsequent cycles would be desirable, reminiscent of molecular ratchets [55]. Also, inhomogeneous distributions of grafted polymers could directly define a net direction of motion.

These approaches, of course, can be combined with techniques that have already been applied to other systems, such as pre-shaping the polymer surface by splitting it to into 'channels' or 'wells', thus constraining the direction of motion. Together with establishing directed motion of single particles, a wealth of further applications of our approach is conceivable. A great advantage compared to existing approaches, i.e. physical pushing of nano-objects, the topography induced movement can be applied in parallel, so that very large numbers of nano-objects could be moved simultaneously. For example, the dependence of the transport properties on particle size suggests to establish a facility in which nano-objects are sorted according to shape and size. The same scheme should also apply to particles of different surface chemistry.

Acknowledgements

We thank Dr Ayothi Ramakrishnan for synthesis of p(MMA-*b*-GMA) diblock-copolymer brushes, Selvaraj Munirasu for the synthesis of p(BnMA-*b*-S) diblock-copolymer brushes, Dr Haining Zhang for the synthesis of PMMA-PGMA mixed brushes, Dr J.D. Jeyaprakash S. Samuel for providing us with the silica nanoparticles, Alexey Kopyshev for AFM measurements, and Dr Mark Santer for useful and stimulating discussions. This work was supported by the Deutsche Forschungsgemeinschaft and the Landesstiftung Baden-Württemberg, Germany.

References

[1] Pincus P. Macromolecules 1991;24:2912.
[2] Ito Y, Ochiai Y, Park YS, Imanishi Y. J Am Chem Soc 1997;119:1619.
[3] Galaev I, Mattiasson B. Trends Biotechnol 1999;17:335.
[4] Aksay A, Trau M, Manne S, Honma I, Yao N, Zhou L, Fenter F, Eisenberger PM, Gruner SM. Science 1996;273:892.
[5] Leger L, Raphael E, Hervert H. Adv Polym Sci 1999;138:185.
[6] Mansky P, Liu Y, Huang E, Russell TP, Hawker CJ. Science 1997;275:1458.
[7] Ruths M, Johannsmann D, Rühe J, Knoll W. Macromolecules 2000;33:3860.
[8] Prokhorova SA, Kopyshev A, Ramakrishnan A, Zhang H, Rühe J. Nanotechnology 2003;14(10):1098.
[9] de Gennes PG. J de Physique 1976;37:1445.

[10] (a) Hadziioannou G, Patel S, Granick S, Tirrell M. J Am Chem Soc 1986;108:2869.
(b) Belder GF, ten Brinke G. Langmuir 1997;13:4102.
[11] Halperin A, Tirrell M, Lodge TP. Adv Polym Sci 1992;100:31.
[12] Alexander SJ. J Phys (Paris) 1977;38:983.
[13] Milner ST, Witten TA, Cates ME. Macromolecules 1989;22:853.
[14] Rühe J, Knoll W. In: Ciferri A, editor. Supramolecular polymers. New York: Marcel Dekker; 2000. p. 565–613. P-00-99.
[15] Milner ST. Europhys Lett 1988;7:695.
[16] Zhulina EB, Borisov OV, Pryamitsyn VA, Birshtein TM. Macromolecules 1991;24:140.
[17] (a) Prucker O, Rühe J. Macromolecules 1998;31:602.
(b) Prucker O, Rühe J. Macromolecules 1998;31:592.
(c) Minko S, Gafijchuk G, Sidorenko A, Voronov S. Macromolecules 1999;32:4525.
(d) Luzinov I, Julthongpiput D, Liebmann-Vinson A, Cregger T, Foster MD, Tsukruk VV. Langmuir 2000;16:504.
[18] Wang JS, Matyjaszewski K. Macromolecules 1995;28:7901.
[19] (a) Advincula RC, Brittain WJ, Rühe J, Caster K. Polymer brushes. New York: Wiley; 2004.
(b) Zhao B, Brittain WJ. Prog Polym Sci, 2000;25:677.
(c) Pyun J, Kowalewski T, Matyjaszewski K. Macromol Rapid Commun, 2003;24:1043.
[20] Dong H, Marko JF, Witten TA. Macromolecules 1994;27:6428.
[21] Brown G, Chakrabarti A, Marko JF. Europhys Lett 1994;25:239.
[22] Zhulina EB, Singh C, Balazs AC. Macromolecules 1996;29:6338.
[23] Matyjaszewski K, Patten TE, Xia JH. J Am Chem Soc 1997;119:674.
[24] Zhao B, Brittain WJ. J Am Chem Soc 1999;121:3557.
[25] Zhao B, Brittain WJ, Zhou W, Cheng SZD. J Am Chem Soc 2000; 122:2407.
[26] Boyes SG, Brittain WJ, Weng X, Cheng SZD. Macromolecules 2002; 35:4960.
[27] Zhao B, Brittain WJ, Zhou W, Cheng SZD. Macromolecules 2000;33: 8821.
[28] Lemieux M, Usov D, Minko S, Stamm M, Shulha H, Tsukruk VV. Macromolecules 2003;36:7244.
[29] Motornov M, Minko S, Eichhorn K-J, Nitschke M, Simon F, Stamm M. Langmuir 2003;19:8077.
[30] Minko S, Müller M, Usov D, Scholl A, Froeck C, Stamm M. Phys Rev Lett 2002;88:035501–035502.
[31] Marko JF, Witten TA. Phys Rev Lett 1991;66:1541.
[32] Müller M. Phys Rev E 2002;65:30802.
[33] Currie EPK, Norde W, Cohen Stuart MA. Adv Colloid Int Sci 2003; 100–102:205.
[34] Kim JU, O'Shaughnessy B. Phys Rev Lett 2002;89:238301.
[35] (a) Colvin VL, Goldstein AN, Alivisatos AP. J Am Chem Soc 1992; 114:5221.
(b) Jiang P, Liu ZF. Appl Phys Lett 1999;75:3023.
(c) Doron A, Katz E, Willner I. Langmuir 1995;11:1313.
(d) Sugimura H, Nakagiri N. J Am Chem Soc 1997;119:9226.
(e) Zheng J, Zhu Z, Chen H, Liu Z. Langmuir 2000;16:4409.
[36] Bhat RR, Genzer J, Chaney BN, Sugg HW, Liebmann-Vinson A. Nanotechnology 2003;14:1145.
[37] Bhat RR, Tomlinson MR, Genzer J. Macromol Rapid Commun 2004; 25:270.
[38] Liu Z, Pappacena K, Cerise J, Kim J, Durning CJ, O'Shaughnessy B, Levicky R. Nano Lett 2002;2:219.
[39] Requicha A. NSF partnership in nanotechnology conference. Jan 29, 2001.
[40] (a) Magnasco MO. Phys Rev Lett 1994;72:2656.
(b) Duke T, Holy TE, Leibler S. Phys Rev Lett 1995;74:330.
[41] (a) Stroscio JA, Eigler DM. Science 1991;254:1319.
(b) Lyo I-W, Avouris P. Science 1991;253:173.
(c) Schaefer DM, Reifenberger R, Patil A, Andres RP. Appl Phys Lett 1995;66:1012.
(d) Sheehan P, Lieber CM. Science 1996;272:1158.
(e) Hsieh SC, Meltzer S, Wang CRC, Requicha AAG, Thompson ME, Koel BE. J Phys Chem B 2002;106:231.
(f) Mohamed MB, Volkov V, Link S, El-Sayed MA. Chem Phys Lett 2000;317:517.
[42] (a) Avouris P, Hertel T, Martel R, Schmidt T, Shea HR, Walkup RE. Appl Surf Sci 1999;141:201.
(b) Kolb DM, Ullmann R, Will T. Science 1997;275:1097.
[43] Hess H, Clemmens J, Qin D, Howaed J, Vogel V. Nano Lett 2001;1: 235.
[44] Straropoulos GN, Dialynas TE, Tsironis GP. Phys Lett A 1999;252: 151.
[45] Fennimore AM, Yuzvinsky TD, Han W-Q, Fuhrer MS, Cumings J, Zettl A. Nature 2003;424:408.
[46] Prokhorova S, Kopyshev A, Ramakrishnan A, Rühe J. In: Advincula RC, Brittain WJ, Rühe J, Caster K, editors. Polymer brushes. New York: Wiley; 2004.
[47] Prokhorova S, Kopyshev A, Ramakrishnan A, Zhang H, Rühe J. Abstr Pap Am Chem 2003;S225:672-poly.
[48] Ramakrishnan A, Dhamodharan R, Rühe J. Macromol Rapid Commun 2002;23:612.
[49] Selvaraj M, Dhamodharan R, Rühe J, Santer S. Submitted to Macromolecules.
[50] Prokhorova SA, Kopyshev A, Ramakrishnan A, Zhang H, Rühe J. Proceeding of SPIE, Nanotechnology 2003;30:5118.
[51] Peng B, Johannsmann D, Rühe J. Macromolecules 1999;32:6759.
[52] Santer S, Kopyshev A, Rühe J. Submitted to Langmuir.
[53] Stöber W, Fink A, Bohn E. J Colloid Interface Sci 1968;26:62.
[54] Israelachvili J. Intermolecular and surface forces, 2nd ed 1992.
[55] Ajdari A, Prost JCR. Acad Sci Paris II 1993;315:1635.